



# Mechanical characterization of matrix-induced autologous chondrocyte implantation (MACI<sup>®</sup>) grafts in an equine model at 53 weeks



Darvin J. Griffin<sup>a</sup>, Edward D. Bonnevie<sup>b</sup>, Devin J. Lachowsky<sup>b</sup>, James C.A. Hart<sup>c</sup>, Holly D. Sparks<sup>c</sup>, Nance Moran<sup>e</sup>, Gloria Matthews<sup>e</sup>, Alan J. Nixon<sup>c</sup>, Itai Cohen<sup>d</sup>, Lawrence J. Bonassar<sup>a,b,\*</sup>

<sup>a</sup> Department of Biomedical Engineering, Cornell University, Ithaca, NY, USA

<sup>b</sup> Sibley School of Mechanical & Aerospace Engineering, Cornell University, Ithaca, NY, USA

<sup>c</sup> Comparative Orthopaedics Laboratory, College of Veterinary Medicine, Cornell University, Ithaca, NY, USA

<sup>d</sup> Department of Physics, Cornell University, Ithaca, NY, USA

<sup>e</sup> Genzyme Corporation, Cambridge, MA, USA

## ARTICLE INFO

### Article history:

Accepted 7 April 2015

### Keywords:

Cartilage repair  
MACI  
ACI  
Friction  
Confined compression  
Confocal strain mapping

## ABSTRACT

There has been much interest in using autologous chondrocytes in combination with scaffold materials to aid in cartilage repair. In the present study, a total of 27 animals were used to compare the performance of matrix-assisted chondrocyte implantation (MACI<sup>®</sup>) using a collagen sponge as a chondrocyte delivery vehicle, the sponge membrane alone, and empty controls. A total of three distinct types of mechanical analyses were performed on repaired cartilage harvested from horses after 53 weeks of implantation: (1) compressive behavior of samples to measure aggregate modulus (HA) and hydraulic permeability ( $k$ ) in confined compression; (2) local and global shear modulus using confocal strain mapping; and (3) boundary friction coefficient using a custom-built tribometer. Cartilage defects receiving MACI<sup>®</sup> implants had equilibrium modulus values that were 70% of normal cartilage, and were not statistically different than normal tissue. Defects filled with Maix<sup>™</sup> membrane alone or left empty were only 46% and 51–63% of control, respectively. The shear modulus of tissue from all groups of cartilage defects were between 4 and 10 times lower than control tissue, and range from 0.2 to 0.4 MPa. The average values of boundary mode friction coefficients of control tissue from all groups ranged from 0.42 to 0.52. This study represents an extensive characterization of the mechanical performance of the MACI<sup>®</sup> grafts implant in a large animal model at 53 weeks. Collectively, these data demonstrate a range of implant performance, revealing similar compressive and frictional properties to native tissue, with inferior shear properties.

© 2015 Published by Elsevier Ltd.

## 1. Introduction:

Articular cartilage has limited ability for self-repair, and as such any defects leave the affected joint susceptible to osteoarthritis (Inerot et al., 1978). Both autologous chondrocyte implantation (ACI) and matrix induced autologous chondrocyte implantation (MACI<sup>®</sup>) have been shown to effectively repair full-thickness chondral defects as evidenced by histology and integration (Inerot et al., 1978). ACI involves only the delivery of cells to a cartilage defect. This technique has been used clinically for over two decades. Despite this extensive

record, surgical challenges still persist including graft hypertrophy, the damaging of adjacent tissue by suturing, and graft delamination.

More recently, modified ACI techniques have been developed using a variety of materials to deliver transplanted chondrocytes (Brittberg, 2010). Specifically, matrix-induced autologous chondrocyte implantation (MACI<sup>®</sup>) involves the use of porcine-derived type I/type III collagen bi-layer membrane secured into cartilage defects using fibrin adhesive (Frenkel et al., 1997). MACI<sup>®</sup> grafts eliminate the need for periosteal harvest, help maintain chondrocyte viability and phenotype, and potentially allows for a more even distribution of cells in the defect (Willers et al., 2005).

Despite the widespread clinical use of such techniques, there is relatively little known about the mechanical properties of the tissue that results use of various cartilage repair techniques. Several studies

\* Correspondence to: 149 Weill Hall, Cornell University, Ithaca, NY 14853, USA.  
Tel.: +1 607255 9381.

E-mail address: [lb244@cornell.edu](mailto:lb244@cornell.edu) (L.J. Bonassar).

report compressive properties obtained through indentation (Peterson et al., 2002; Henderson et al., 2007), unconfined (Laasanen et al., 2003), and confined compression tests (Strauss et al., 2005; Peretti et al., 2001). Confined compression testing on ACI repaired equine tissue showed an aggregate modulus that was only 12% of native tissue (Strauss et al., 2005). A MACI graft with a type II collagen membrane was shown to have an aggregate modulus that was 15% of native tissue (Lee et al., 2000). Stiffness tests in an ovine model showed that MACI<sup>®</sup> grafts ranged from 16% to 50% of native cartilage (Russlies et al., 2003; Jones et al., 2008). The duration of implanted tissue ranged from as short as a few weeks to as long as several years. A general trend shown in this data is that longer implant durations tend to perform better, indicating that mechanical properties of repaired cartilage may improve over time.

The current study was motivated by the lack of data on other critical mechanical properties of autologous chondrocyte grafts. For example, there are no published papers that study friction or shear properties of the repaired cartilage in long term large animal models. In this study, we performed an array of mechanical tests to more fully understand the functionality and mechanical behavior of matrix-induced autologous chondrocyte grafts. Therefore, the primary objective of this study was to characterize the compressive, shear, and friction properties of repaired articular cartilage after 53 weeks in an equine model.

## 2. Materials and methods

### 2.1. Chondrocyte isolation and expansion

Cartilage biopsies were obtained arthroscopically from the femoral trochlear ridge of 24 horses. Cartilage samples were enzymatically digested and expanded in vitro before seeding on sterile processed collagen type I/III membranes (ACI-Maix<sup>™</sup>; Genzyme Corporation). Cells were seeded at 0.5 million chondrocytes/cm<sup>2</sup> of collagen membrane, and covered with DMEM and incubated for 48 h before implantation. Additionally, a collagen type I/III membrane was cultured without chondrocytes, for use in control defects implanted with membrane alone.

### 2.2. Implantation surgery

A total of 27 skeletally mature horses (1.5–6 yr of age, 300–400 kg weight) free of lameness were used. Arthroscopy surgeries were performed according to the guidelines of the Institutional Animal Care and Use Committee (IACUC) at Cornell University. Two full-thickness chondral defects (15 mm diameter) were created on the femoral trochlear ridge of one hind-limb of each horse, using a trephine and cannula. These lesions extended down to, but not through, the subchondral bone plate, and resulted in minimal bleeding or seepage of marrow into the defect. Specifically, defects were placed in both the proximal and distal region of the trochlea in either the right or left joint, with the contralateral joint left unoperated for control (Fig. 1). Animals were assigned to one of three cohorts based on treatment provided in each of the two defects: (1) MACI<sup>®</sup> graft in one defect and the carrier scaffold, consisting of the ACI-Maix (Matricel) membrane without the presence of cells in other defect ( $n=12$ ); (2) MACI<sup>®</sup> graft and an empty defect ( $n=12$ ); and (3) both defect sites left empty ( $n=3$ ). The choice of operation on the right or left joint along as well as location within the trochlea was randomized, with all subsequent histological and mechanical analysis performed in a blinded fashion. After 53 weeks, the horses were euthanized and samples were immediately harvested for histological examination and mechanical assessment (Fig. 1).

### 2.3. Histology and immunohistochemistry

Samples were decalcified in hematoxylin and eosin (H&E) or ethylenediaminetetraacetic acid (EDTA) and sectioned at 6  $\mu\text{m}$ , as previously described (Nixon et al., 2011). Sections were stained with toluidine blue for histochemical reaction to cartilage GAG moieties. Serial sections were used for positive and negative reactions for collagen type II immunohistochemistry (Nixon et al., 2011).

### 2.4. Confined compression

A total of 108 full thickness cylindrical plugs (3 mm diameter) were harvested from the defect region using a biopsy punch perpendicular to the articular surface. The plugs were thawed in a bath of phosphate buffer saline (PBS) containing protease

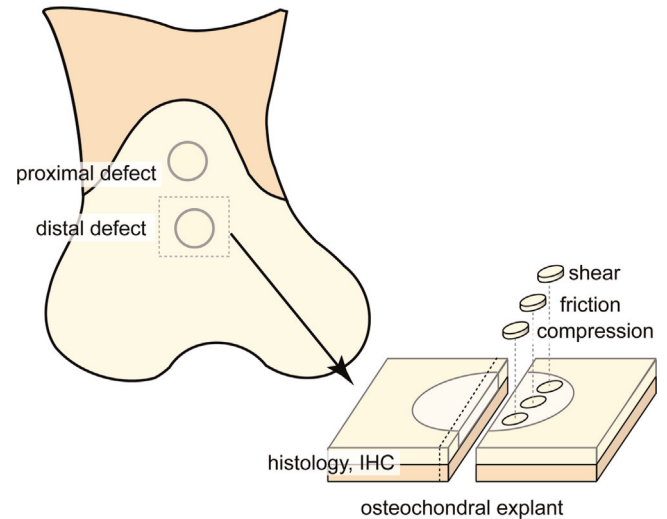


**Fig. 1.** Two 15 mm defects are placed into the trochlea of the right or left limb of each horse and either left empty, or filled with MAIX membrane or MACI graft. Osteochondral blocks were extracted after sacrifice with sections taken for histology containing both repair and local tissue and 3 mm plugs taken for each of shear, friction, and compression testing.

inhibitors. This procedure was repeated for samples harvested from the proximal and distal region of the trochlea in the control joint. Prior to testing, sample heights were measured using a caliper. Samples were placed in a 3 mm confining chamber, covered with a porous plug and PBS with protease inhibitors, and mounted in a Bose EnduraTEC ELF 3200 for stress–relaxation testing. A series of 5% steps in compressive strain were imposed on each sample up to a total of 40% strain. For each step, the resultant load was measured for 10 min using a Honeywell 50 lb load cell at a frequency of 1 Hz. The stress–relaxation curves were fit to a poroelastic model and analyzed using custom MATLAB code to calculate aggregate modulus (Ha) and hydraulic permeability ( $k$ ) (Gleghorn et al., 2007; Chang et al., 2001).

### 2.5. Friction testing

A total of 84 full thickness cylindrical plugs (3 mm diameter) were tested in a custom tribometer to measure boundary friction coefficients as previously described (Bonnieville et al., 2014; Gleghorn et al., 2007; Gleghorn et al., 2010; Galley et al., 2011). Samples were linearly reciprocated against glass at a speed of 0.1 mm/s under 40% strain while bathed in PBS, conditions known to induce boundary mode lubrication. During sliding, both normal and shear forces were collected to determine the friction coefficient. The friction coefficient was calculated by averaging shear force divided by normal force, for both directions of sliding.

### 2.6. Shear confocal strain mapping

A total of 84 full thickness cylindrical plugs (3 mm diameter) were prepared for confocal strain mapping as described previously (Griffin et al., 2014; Buckley et al., 2008, 2010, 2012; Silverberg et al., 2013). Samples were bisected longitudinally into hemi-cylinders, exposed to 7  $\mu\text{g}/\text{mL}$  5-dichlorotriazinyl-aminofluorescein (5-DTAF) for 2 h to uniformly stain the extracellular matrix, and rinsed in PBS for 30 min. Briefly, samples were glued to a tissue deformation imaging stage (TDIS) and compressed to 10% strain. The TDIS was mounted on an inverted Zeiss LSM 510 5 Live confocal microscope and imaged using a 488 nm laser. A line perpendicular to the articular surface was photobleached using the laser at full intensity. Sinusoidal shear displacements were placed on the articular surface by the TDIS at a frequency of 0.1 Hz and amplitude of 16  $\mu\text{m}$ , and the resultant forces were measured with a load cell. Simultaneously, images of the sample deforming were collected at 10 frames per second. Using custom MATLAB code, the intensity minima corresponding to the location of the photobleached line was tracked, and the local strains

were determined from the slopes of that line. The local shear modulus ( $G$ ) was calculated from the local strain and measured load.

### 2.7. Statistical analysis

For the confined compression tests, each defect was matched to a contralateral control in the opposite joint. Comparison between repair groups and corresponding contralateral controls was performed using a two-tailed paired  $t$ -test with bonferroni correction. Minimum detectable differences between control and repaired cartilage were calculated based on sample size, the standard deviation of repaired cartilage, and assuming a power of 0.8. For both friction and confocal strain mapping, it was not possible to harvest a defect sample from every joint. Therefore, a standard two-tailed  $t$ -test assuming unequal sample variance between groups was used to analyze the repair groups to control. For all mechanical tests, a one-way analysis of variance (ANOVA) test was performed between all testing groups. Finally, the MACI<sup>®</sup> group and empty group were compared using a two-tailed  $t$ -test. All data groups are displayed as mean values with standard deviations noted by error bars. Differences were considered significant for  $p < 0.05$ .

## 3. Results

### 3.1. Histology and immunohistochemistry

H&E stain revealed improved filling and attachment of MACI<sup>®</sup> implants compared to cell free ACI-Maix implants and spontaneous healing in the empty defect (Fig. 2). Toluidine blue reactive cartilage was thicker in MACI<sup>®</sup> implanted defects, compared to Maix or empty defects. Similarly, collagen type II was more abundant in MACI<sup>®</sup> implanted defects, compared to empty defects.

### 3.2. Confined compression

Cartilage from defects receiving MACI<sup>®</sup> implants had an equilibrium modulus that was 70% of normal cartilage, which was not statistically different than native control tissue ( $p=0.07$ ) (Fig. 3A). Based on power calculations, the minimum detectable difference between groups was 0.23 MPa which was lower than the difference between the MACI<sup>®</sup> and control moduli (0.31 MPa). Defects filled with ACI-Maix<sup>™</sup> membrane alone or left empty had equilibrium moduli that were 46% ( $p < 0.05$ ) and 59% ( $p < 0.05$ ) of control, respectively. The hydraulic permeability of tissue from MACI<sup>®</sup> grafts were 2.6–7.0 times higher than control tissue, but were not statistically different from control (Fig. 3B). Hydraulic permeability of

groups with ACI-Maix<sup>™</sup> membrane alone were 2.5 times higher than control, but were less varied, and as a result were statistically different from controls. Empty defects had 2.3–6.6 times higher hydraulic permeability values than controls, with only one group statistically different.

### 3.3. Coefficient of friction

The average values of boundary mode friction coefficients of control tissue and from all implant groups ranged from 0.42 to 0.52 with no statistical difference between groups (Fig. 4A).

### 3.4. Confocal strain mapping

The global values of shear modulus for control cartilage ranged from 1.0 to 1.5 MPa, consistent with previous data (Griffin et al., 2014; Buckley et al., 2008, 2010, 2012; Silverberg et al., 2013) (Fig. 4B). The shear moduli of tissue from all groups of cartilage defects were 4–10 times lower than control cartilage, and ranged between 0.2 and 0.5 MPa ( $p < 0.05$ ). The local shear modulus of the control cartilage showed variation with depth, with the minimum modulus value occurring within 100  $\mu\text{m}$  of the articular surface (Fig. 5A–C). In contrast, local shear moduli of the repaired cartilage defects were significantly lower than control tissue, showing no minimum or variation with depth. Next we compared the moduli for  $G_{\text{min}}$  (averaged 50–150  $\mu\text{m}$ ) and  $G_{\text{plateau}}$  (200–1000  $\mu\text{m}$ ) values for defect and control groups (Fig. 5D–F). We found  $G_{\text{min}}$  for cartilage defects was 1.5–2 times lower than that for control cartilage, whereas the  $G_{\text{plateau}}$  values were 7–10 times lower than those of native tissues (Fig. 5D–F).

## 4. Discussion

The goal of the present study was to provide a more thorough characterization of the mechanical performance of repaired cartilage implants than has been reported previously. MACI<sup>®</sup> implants were tested in a large animal defect model for over 1 yr, and revealed overall better defect filling, toluidine blue reactive matrix, and collagen type II staining compared to ACI-Maix<sup>™</sup> membranes alone or paired empty defects. Furthermore, a total of 276 samples harvested from implants and controls were tested to measure friction, compressive, and shear properties. These data show a range in implant performance, with frictional properties of all implants similar to control, compressive modulus of MAIX<sup>™</sup> and empty implants were different from controls, and shear properties for all groups that differed significantly from controls. Previous research involving the mechanical performance of MACI grafts report average compressive stiffness values ranging from

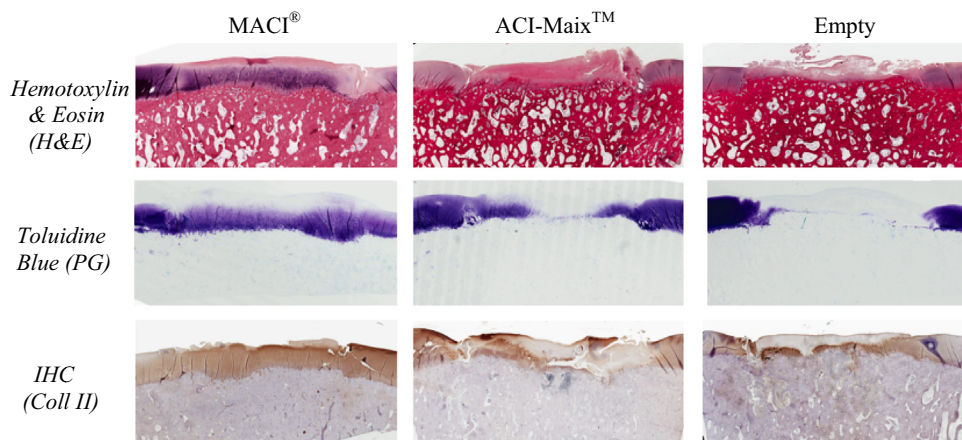
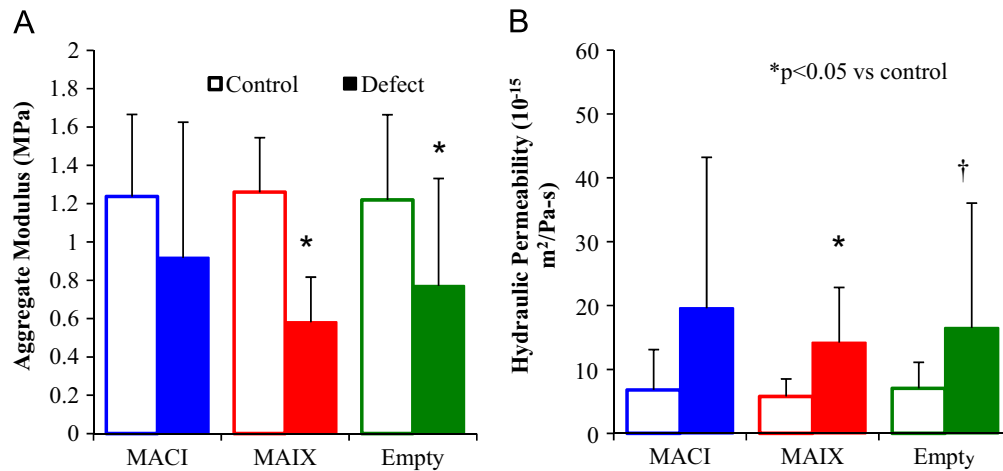
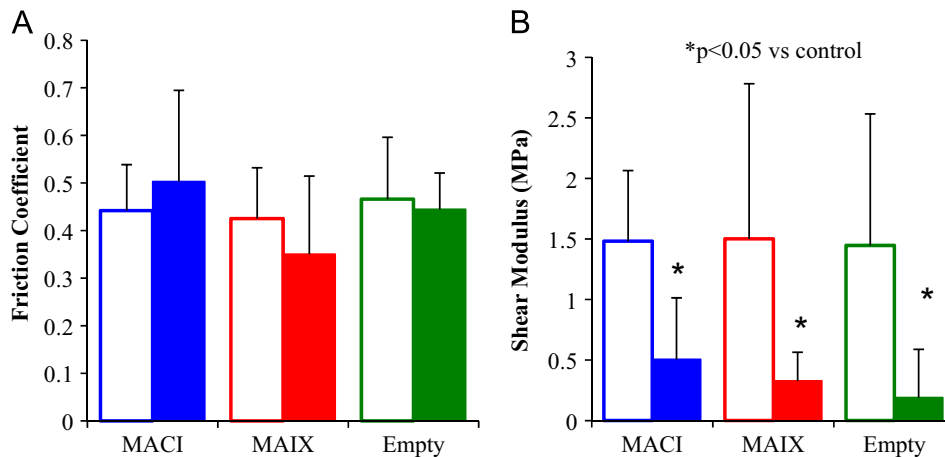


Fig. 2. Histological and immunohistochemical photomicrographs of MACI<sup>®</sup>, ACI-Maix (cell-free), and empty implanted defects 53 weeks after repair.



**Fig. 3.** Average (A) aggregate modulus and (B) hydraulic permeability for each group and its contralateral control. All values expressed as mean  $\pm$  standard deviation ( $n=12$  for groups MACI and MAIX,  $n=6$  for group Empty). \* $p < 0.05$  vs. native control tissue, † one group statistically different.



**Fig. 4.** Average (A) boundary mode friction coefficients (B) global shear modulus for each group and its contralateral control. All values expressed as mean  $\pm$  standard deviation ( $n=12$  for control groups MACI & MAIX,  $n=6$  for control group empty,  $n=15, 5, 10$  for defect groups in order). \* $p < 0.05$  vs. native control tissue.

16% to 50% of native cartilage. In our confined compression testing, defects filled with MACI<sup>®</sup> grafts performed relative to their contralateral control (70%). The average aggregate modulus and hydraulic permeability of the MACI<sup>®</sup> groups were not statistically different than the control tissue (Fig. 3A,B). The MACI<sup>®</sup> grafts in this study had an aggregate modulus that was 70% of native cartilage on average. Some of the increased performance of these MACI<sup>®</sup> grafts may be attributed to the long-term implant duration and the use of a large animal model.

The healthy function of engineered or repaired tissue and its contacting body (i.e. the apposing meniscus or cartilage), may be dependent on providing a low friction surface during articulation (Gleghorn et al., 2010; Lane, Healey, et al., 2009; Neu et al., 2008). Consequently, researchers have turned towards different mechanical and chemical stimuli during pre-implantation culture to promote effective lubrication (Grad et al., 2012; Huang et al., 2012; Bonnevie et al., 2014). Previously, in vitro studies have shown that although frictional properties of tissue repair scaffolds can be significantly higher than native cartilage, the localization of lubricants on the scaffolds can effectively reduce friction coefficients (Bonnevie et al., 2014; Gleghorn et al., 2007; Singh et al., 2014; Bhumiratana et al., 2014). Similarly, in a meniscus repair study, scaffolds that were tested before and after in vivo implantation exhibited progressively lower friction coefficients as a function of implant time (Gleghorn et al., 2010; Galley et al., 2011). In this study, the tribological characterization revealed no significant differences between all sample groups

and native cartilage. Such data are consistent with the idea that at one year of implantation, these implants are sufficiently capable of localizing boundary lubricants to enable functional lubrication.

During confocal strain mapping, defects performed significantly worse than their contralateral normal controls, regardless of treatment condition (Fig. 4B). Local spatial shear profiles revealed the depth dependent modulus for control and repaired tissue (Fig. 5). Control tissue showed large variation of modulus in depth; while, engineered tissue showed 4–10 times lower modulus in both the minimum and plateau moduli.

The low shear modulus of the all grafts makes any repaired cartilage susceptible to mechanical failure or degradation. Previous studies have shown that shear properties of normal cartilage are highly dependent on collagen content and organization (Buckley et al., 2012; Palmer, et al., 2009). Tissue from repaired cartilage defects is known to have different collagen fiber size and organization compared to normal tissue (Griffin et al., 2014), which is consistent with our current observations that global and local shear properties do not match native tissue. It can be noted that the reduction in  $|G^*|$  arises from lack of organized collagen within repaired tissue grafts; this is consistent with predictions of network-based models of crosslinked polymers (Silverberg et al., 2014). These models predict that below critical values of fiber concentration, size, and connectivity, shear modulus is very low. Only after the percolation threshold is achieved does shear modulus increase dramatically. Based on the data in the current study, it seems likely that



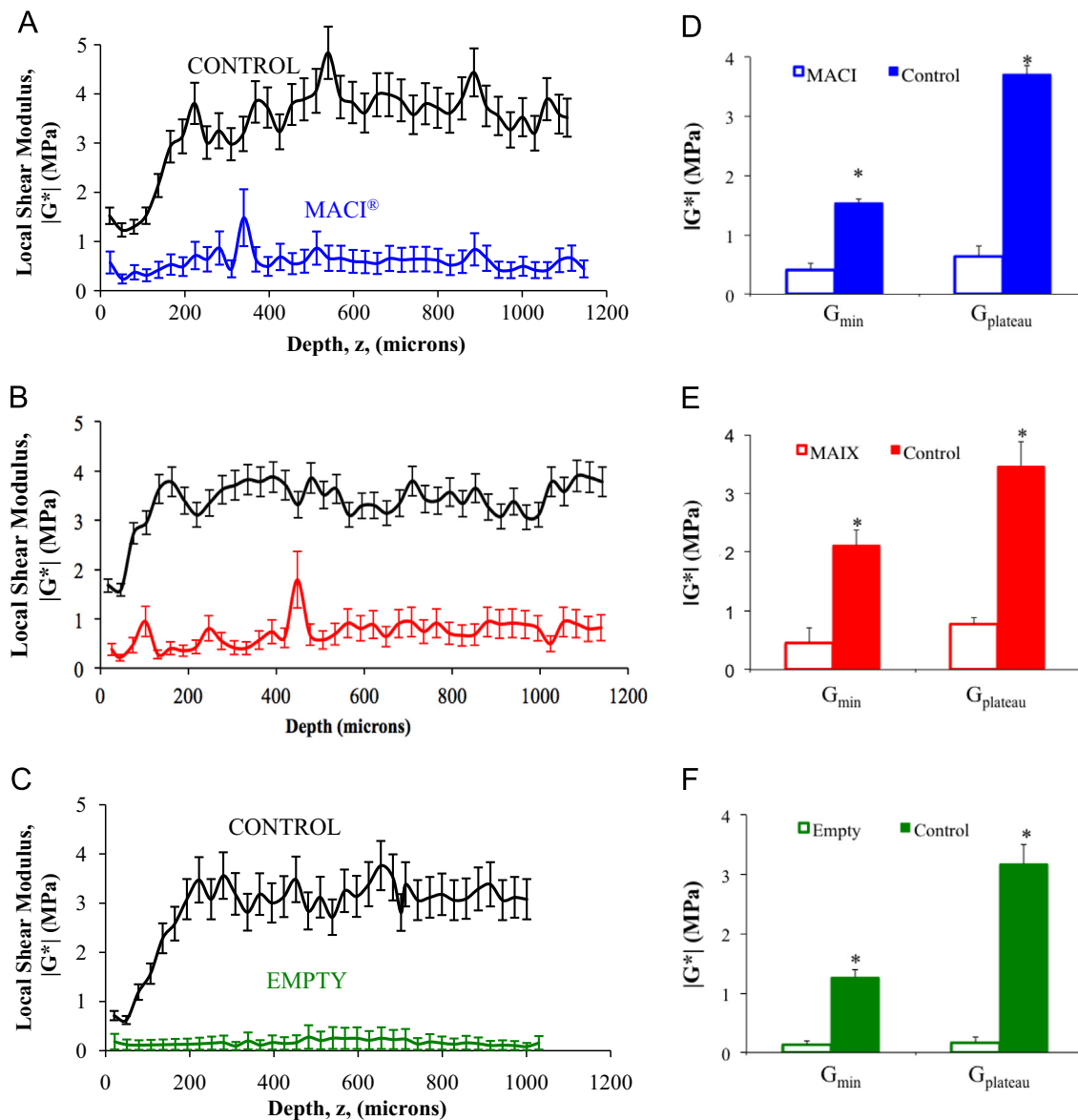


**Fig. 5.** (A–C) Local shear modulus profiles for tissue samples harvested from each of the implant groups tested. (D–F)  $G_{min}$  (averaged 50–150  $\mu\text{m}$ ) and  $G_{plateau}$  (averaged 200–1000  $\mu\text{m}$ ) values for defect and control groups. \* $p < 0.001$  vs. native control tissue.

repaired cartilage in all groups is a loose, discontinuous collagen network that is near the rigidity percolation threshold. As such, ensuring sufficient collagen concentration, size, and connectivity may be of particular importance for improving cartilage repair and overall performance of any cartilage repair procedure.

MACI<sup>®</sup> implants show promise for repairing osteochondral defects and in matching compressive and frictional properties of native cartilage; however, attention should be focused on improving the shear properties of such implants. The results underscore that histologic assessment and biochemical analysis alone are not sufficient for predicting the mechanical performance of cartilage grafts. Histologic analysis displayed that MACI<sup>®</sup> grafts (Fig. 2) improved chondrocyte proliferation and GAG content over empty defects, however, biomechanical benefit was only evident in aggregate modulus and hydraulic permeability (Fig. 3) and not in the shear properties (Fig. 5). The relationship between structure and function is quite complex in repaired tissue and may differ even from that of native cartilage. As such, thorough mechanical evaluation of such implants is critical to assess the performance of repaired cartilage.

#### Disclosure of conflicts of interest

Nance Moran and Gloria Matthews are full-time employees of Genzyme Corporation, a Sanofi Company located in Cambridge, MA. Darwin J. Griffin and Edward D. Bonnevie received financial support through National Science Foundation fellowships. Alan J. Nixon, James Hart, Holly Sparks, Devin Lachowsky, Itai Cohen, and Lawrence J. Bonassar received funding to support through work from Genzyme Corporation through a sponsored research agreement with Cornell University.

#### Acknowledgments

The authors gratefully acknowledge Natalie Galley and Jessie Silverberg for their discussions and contributions. This work was supported by Genzyme Corporation, Cornell University, Diversity Programs in Engineering, Cornell Veterinary Medicine, and the National Science Foundation Graduate Research Fellowship.

## References

- Bhumiratana, S., Eton, R.E., Oungoulian, S.R., Wan, L.Q., Ateshian, G.A., Vunjak-Novakovic, G., 2014. Large, stratified, and mechanically functional human cartilage grown in vitro by mesenchymal condensation. *Proc. Natl. Acad. Sci. U.S.A.* 111 (19), 6940–6945. <http://dx.doi.org/10.1073/pnas.1324050111>.
- Bonnevie, E.D., Puetzler, J.L., Bonassar, L.J., 2014. Enhanced boundary lubrication properties of engineered menisci by lubricin localization with insulin-like growth factor I treatment. *J. Biomech.* 47 (9), 2183–2188. <http://dx.doi.org/10.1016/j.jbiomech.2013.10.028>.
- Brittberg, M., 2010. Cell carriers as the next generation of cell therapy for cartilage repair: a review of the matrix-induced autologous chondrocyte implantation procedure. *Am. J. Sports Med.* 38 (6), 1259–1271. <http://dx.doi.org/10.1177/0363546509346395>.
- Buckley, M.R., Bergou, A.J., Fouchard, J., Bonassar, L.J., Cohen, I., 2010. High-resolution spatial mapping of shear properties in cartilage. *J. Biomech.* 43 (4), 796–800. <http://dx.doi.org/10.1016/j.jbiomech.2009.10.012>.
- Buckley, M.R., Bonassar, L.J., Cohen, I., 2012. Localization of viscous behavior and shear energy dissipation in articular cartilage under dynamic shear loading. *J. Biomech. Eng.* 135 (3), 31002. <http://dx.doi.org/10.1115/1.4007454>.
- Buckley, M.R., Gleghorn, J.P., Bonassar, L.J., Cohen, I., 2008. Mapping the depth dependence of shear properties in articular cartilage. *J. Biomech.* 41 (11), 2430–2437. <http://dx.doi.org/10.1016/j.jbiomech.2008.05.021>.
- Chang, S.C., Rowley, J.A., Tobias, G., Genes, N.G., Roy, A.K., Mooney, D.J., Bonassar, L.J., 2001. Injection molding of chondrocyte/alginate constructs in the shape of facial implants. *J. Biomed Mater. Res.* 55 (4), 503–511 (<http://www.ncbi.nlm.nih.gov/pubmed/11288078>).
- Frenkel, S.R., Toolan, B., Menche, D., Pitman, M.I., Pachence, J.M., 1997. Chondrocyte transplantation using a collagen bilayer matrix for cartilage repair. *J. Bone Jt. Surg. Br. Vol.* 79 (5), 831–836 (<http://www.ncbi.nlm.nih.gov/pubmed/9331046>).
- Galley, N.K., Gleghorn, J.P., Rodeo, S., Warren, R.F., Maher, S.A., Bonassar, L.J., 2011. Frictional properties of the meniscus improve after scaffold-augmented repair of partial meniscectomy: a pilot study. *Clin. Orthop. Relat. Res.* 469 (10), 2817–2823. <http://dx.doi.org/10.1007/s11999-011-1854-6>.
- Gleghorn, J.P., Doty, S.B., Warren, R.F., Wright, T.M., Maher, S.A., Bonassar, L.J., 2010. Analysis of frictional behavior and changes in morphology resulting from cartilage articulation with porous polyurethane foams. *J. Orthop. Res.: Off. Publ. Orthop. Res. Soc.* 28 (10), 1292–1299. <http://dx.doi.org/10.1002/jor.21136>.
- Gleghorn, J.P., Jones, A.R.C., Flannery, C.R., Bonassar, L.J., 2007. Boundary mode frictional properties of engineered cartilaginous tissues. *Eur. Cells Mater.* 14, 20–28 (discussion 28–29) (<http://www.ncbi.nlm.nih.gov/pubmed/17676563>).
- Grad, S., Loparic, M., Peter, R., Stolz, M., Aebi, U., Alini, M., 2012. Sliding motion modulates stiffness and friction coefficient at the surface of tissue engineered cartilage. *Osteoarthr. Cartil.* 20 (4), 288–295. <http://dx.doi.org/10.1016/j.joca.2011.12.010>.
- Griffin, D.J., Vicari, J., Buckley, M.R., Silverberg, J.L., Cohen, I., Bonassar, L.J., 2014. Effects of enzymatic treatments on the depth-dependent viscoelastic shear properties of articular cartilage. *J. Orthop. Res.: Off. Publ. Orthop. Res. Soc.* 32 (12), 1652–1657. <http://dx.doi.org/10.1002/jor.22713>.
- Henderson, I., Lavigne, P., Valenzuela, H., Oakes, B., 2007. Autologous chondrocyte implantation: superior biologic properties of hyaline cartilage repairs. *Clin. Orthop. Relat. Res.* 455, 253–261. <http://dx.doi.org/10.1097/01.blo.0000238829.42563.56>.
- Huang, A.H., Baker, B.M., Ateshian, G.A., Mauck, R.L., 2012. Sliding contact loading enhances the tensile properties of mesenchymal stem cell-seeded hydrogels. *Eur. Cells Mater.* 24, 29–45 (<http://www.ncbi.nlm.nih.gov/pubmed/22791371>).
- Inerot, S., Heinegård, D., Audell, L., Olsson, S.E., 1978. Articular-cartilage proteoglycans in aging and osteoarthritis. *Biochem. J.* 169 (1), 143–156 (<http://www.pubmedcentral.nih.gov/articlerender.fcgi?artid=1184203&tool=pmcentrez&rendertype=abstract>).
- Jones, C.W., Willers, C., Keogh, A., Smolinski, D., Fick, D., Yates, P.J., Zheng, M.H., 2008. Matrix-induced autologous chondrocyte implantation in sheep: objective assessments including confocal arthroscopy. *J. Orthop. Res.: Off. Publ. Orthop. Res. Soc.* 26 (3), 292–303. <http://dx.doi.org/10.1002/jor.20502>.
- Laasanen, M.S., Töyräs, J., Vasara, A.L., Hyttinen, M.M., Saarakkala, S., Hirvonen, J., Kiviranta, I., 2003. Mechano-acoustic diagnosis of cartilage degeneration and repair. *J. Bone Jt. Surg. Am. Vol.* 85-A, S78–S84 (<http://www.ncbi.nlm.nih.gov/pubmed/9331046>).
- Lane, J., Healey, R., Amiel, D., 2009. Changes in condylar coefficient of friction after osteochondral graft transplantation and modulation with hyaluronan. *Arthrosc.: J. Arthrosc. & Relat. Surg.: Off. Publ. Arthrosc. Assoc. N. Am. Int. Arthrosc. Assoc.* 25 (12), 1401–1407. <http://dx.doi.org/10.1016/j.arthro.2009.04.074>.
- Lee, C.R., Grodzinsky, A.J., Hsu, H.P., Martin, S.D., Spector, M., 2000. Effects of harvest and selected cartilage repair procedures on the physical and biochemical properties of articular cartilage in the canine knee. *J. Orthop. Res.: Off. Publ. Orthop. Res. Soc.* 18 (5), 790–799. <http://dx.doi.org/10.1002/jor.1100180517>.
- Neu, C.P., Komvopoulos, K., Reddi, A.H., 2008. The interface of functional biotribology and regenerative medicine in synovial joints. *Tissue Eng. Part B, Rev.* 14 (3), 235–247. <http://dx.doi.org/10.1089/ten.teb.2008.0047>.
- Nixon, A.J., Begum, L., Mohammed, H.O., Huibregtse, B., O'Callaghan, M.M., Matthews, G.L., 2011. Autologous chondrocyte implantation drives early chondrogenesis and organized repair in extensive full- and partial-thickness cartilage defects in an equine model. *J. Orthop. Res.: Off. Publ. Orthop. Res. Soc.* 29 (7), 1121–1130. <http://dx.doi.org/10.1002/jor.21366>.
- Palmer, A.W., Wilson, C.G., Baum, E.J., Levenston, M.E., 2009. Composition-function relationships during IL-1-induced cartilage degradation and recovery. *Osteoarthr. Cartil.* 17 (8), 1029–1039. <http://dx.doi.org/10.1016/j.joca.2009.02.009>.
- Peretti, G.M., Randolph, M.A., Zaporojan, V., Bonassar, L.J., Xu, J.W., Fellers, J.C., Yaremchuk, M.J., 2001. A biomechanical analysis of an engineered cell-scaffold implant for cartilage repair. *Ann. Plast. Surg.* 46 (5), 533–537 (<http://www.ncbi.nlm.nih.gov/pubmed/11352428>).
- Peterson, L., Brittberg, M., Kiviranta, I., Akerlund, E.L., Lindahl, A., 2002. Autologous chondrocyte transplantation. *Biomechanics and long-term durability.* *Am. J. Sports Med.* 30 (1), 2–12 (<http://www.ncbi.nlm.nih.gov/pubmed/11798989>).
- Russlies, M., Rütger, P., Köller, W., Stomberg, P., Behrens, P., 2003. Biomechanical properties of cartilage repair tissue after different cartilage repair procedures in sheep. *Z. Für Orthop. Ihre Grenzgeb.* 141 (4), 465–471. <http://dx.doi.org/10.1055/s-2003-41560>.
- Silverberg, J.L., Barrett, A.R., Das, M., Petersen, P.B., Bonassar, L.J., Cohen, I., 2014. Structure–function relations and rigidity percolation in the shear properties of articular cartilage. *Biophys. J.* 107 (7), 1721–1730. <http://dx.doi.org/10.1016/j.bpj.2014.08.011>.
- Silverberg, J.L., Dillavou, S., Bonassar, L., Cohen, I., 2013. Anatomic variation of depth-dependent mechanical properties in neonatal bovine articular cartilage. *J. Orthop. Res.: Off. Publ. Orthop. Res. Soc.* 31 (5), 686–691. <http://dx.doi.org/10.1002/jor.22303>.
- Singh, A., Corvelli, M., Unterman, S.A., Wepasnick, K.A., McDonnell, P., Elisseeff, J.H., 2014. Enhanced lubrication on tissue and biomaterial surfaces through peptide-mediated binding of hyaluronic acid. *Nat. Mater.* 13 (10), 988–995. <http://dx.doi.org/10.1038/nmat4048>.
- Strauss, E.J., Goodrich, L.R., Chen, C.-T., Hidaka, C., Nixon, A.J., 2005. Biochemical and biomechanical properties of lesion and adjacent articular cartilage after chondral defect repair in an equine model. *Am. J. Sports Med.* 33 (11), 1647–1653. <http://dx.doi.org/10.1177/0363546505275487>.
- Willers, C., Chen, J., Wood, D., Xu, J., Zheng, M.H., 2005. Autologous chondrocyte implantation with collagen bioscaffold for the treatment of osteochondral defects in rabbits. *Tissue Eng.* 11 (7–8), 1065–1076. <http://dx.doi.org/10.1089/ten.2005.11.1065>.